Materials Research Proceedings 33 (2023) 213-218 https://doi.org/10.21741/9781644902677-31

Time domain aeroelastic analysis of wing structures by means of an alternative aeroelastic beam approach

Carmelo Rosario Vindigni[1,a*]

[1]University of Enna Kore, Faculty of Engineering and Architecture, 94100, Cittadella Universitaria, Enna, Italy

[a]carmelorosario.vindigni@unikore.it

Keywords: Aeroelastic Beam, Wing Stick Model, Wing-Aileron Flutter

Abstract. In this work an alternative beam finite element for rapid time-domain flutter analysis of wings equipped with trailing edge control surfaces, generally distributed along the span, is presented. The aeroelastic beam finite element proposed is based on Euler-Bernoulli beam theory, De St. Venant torsion theory and two-dimensional time-domain unsteady aerodynamics. The developed finite element model is attractive for preliminary aero-servo-elastic analyses and flutter suppression systems design purposes; moreover, the finite element matrices obtained could be easily included in existing aeroelastic optimization codes that already use beam modelling of lifting structures to carry out aeroelastic tailoring studies.

Introduction

In modern design of wing structures energy and cost saving considerations have become more important leading to the preference of lightweight structural configurations. Anyway, lightweight structures suffer of susceptibility to aeroelastic instabilities. The simplest aeroelastic model that can be used for preliminary aeroelastic analysis is the three degrees of freedom 3DOF model proposed by Theodorsen that reduces the wing structure to its representative mean airfoil and implements the structural stiffnesses by means of heave, torsional, and flap hinge springs [1]. Anyway, though the 3DOF system is representative of high aspect ratio HAR wings with full-span trailing edge control surfaces, it is not best suited for aero-servo-elastic analysis of wings with considerable variations in stiffness and mass balance along the span or wings that presents locally distributed control surfaces. Nowadays the most popular design and verification tool for aeroelastic analysis of wing structures is the combination of the Finite Element Method FEM, used to model the structural system, coupled with the Doublet Lattice Method DLM, used to model the aerodynamic system, and the connection between structure and aerodynamics is performed by means of splines [2]. Unfortunately, this kind of aeroelastic model presents high computational costs and it is better suitable for the verification phase of the project than for the preliminary assessment phase of the design. A widely used method for preliminary aeroelastic analysis of wings is based on the realization of equivalent beam models of the structure, that can be coupled with different aerodynamic models such as the strip theory and the unsteady vortex lattice method. In this work an alternative modelling approach based on an aeroelastic beam finite element formulation is presented and used for preliminary aero-servo-elastic time domain analyses of wings with trailing edge control surfaces. The equivalent beam modelling of the wing is based on Euler-Bernoulli beam assumptions, De St. Venant torsion theory, and 2D unsteady aerodynamics.

Methods

The structural model considered in this work represents a cantilever wing with thin symmetric airfoil, straight elastic axis EA, and a trailing edge aileron-like control surface. The wing is inextensible and with an infinite chordwise bending stiffness. The elastic axis of the wing lies on the x axis, identifying the spanwise direction, while the cross section lies in the y-z plane, where

Materials Research Proceedings 33 (2023) 213-318 https://doi.org/10.21741/9781644902677-31

y and z are oriented in the positive flow and upwards directions, respectively. The aileron control surface is hinged to the wing frame and connected to the actuators that provide a local stiffness k_{act}, it is also considered aerodynamically unbalanced; moreover, the aileron is considered flexible in torsion and with elastic axis close enough to the hinge line such that they could be considered coincident. The wing is modelled as a Euler-Bernoulli beam that also behave in accordance with De Saint Venant torsion theory and presents bending-torsion inertial coupling. The structural degrees of freedom of the wing-stick model are the vertical displacement due to bending w (positive upwards), the elastic torsional rotation ϕ around the elastic axis (positive nose-up), and the control surface rotation δ about its hinge (positive flap down). The wing's geometric parameters of interest are given in Fig. 1.

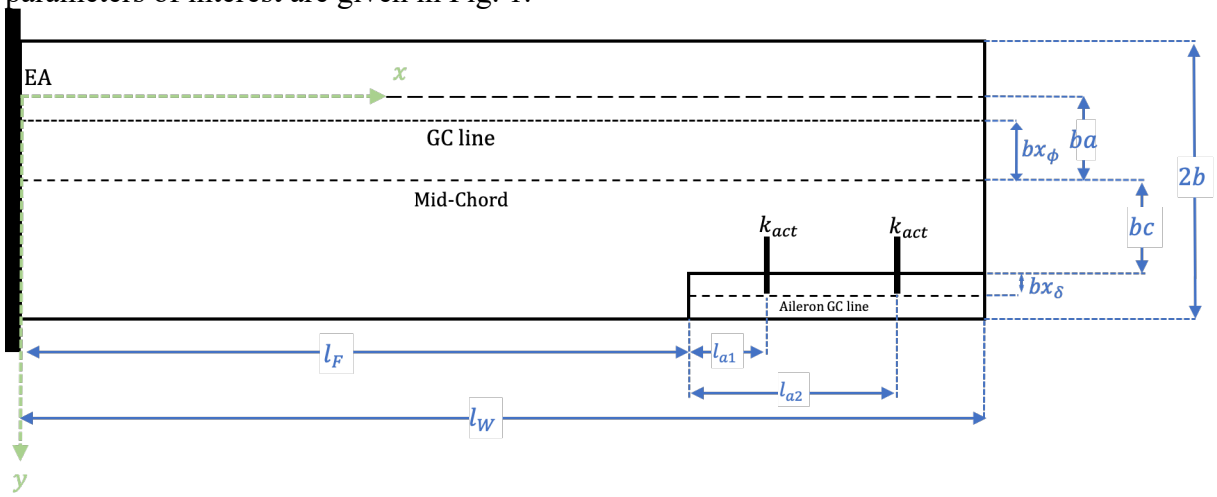

Figure 1 - Wing schematic

The equations of motion of the wing are the ones of a beam with EI bending stiffness and GJ torsional stiffness, while the torsional governing equation of the flap is the one of a beam with a combined torsional stiffness given by the sum of its elastic stiffness $G_f J_f$ and the hinge stiffness K_δ. The loads acting on the beam are given by the unsteady aerodynamic modelling provided by Theodorsen for thin symmetric airfoils undergoing harmonic motion that are written in time domain taking advantage of an indicial function approach [3]. The governing equations of the wing can be written in compact form as [4]

$$[\boldsymbol{M}_s + \boldsymbol{M}_{\text{aer}}]\ddot{\boldsymbol{q}}(t) + [\boldsymbol{C}_s + \boldsymbol{C}_{\text{aer}}]\dot{\boldsymbol{q}}(t) + [\boldsymbol{K}_s\mathcal{D}^2 + \boldsymbol{K}_\delta + \boldsymbol{K}_{\text{aer}}]\boldsymbol{q}(\boldsymbol{t}) = 0. \quad (1)$$

where $\mathbf{q}(\mathbf{t}) = [\text{w} \quad \phi \quad \delta \quad \bar{x}]^{\mathbf{T}}$ is the generalized displacement vector, $\mathbf{M}_s$ and $\mathbf{M}_{\text{aer}}$ are the structural and aerodynamics mass matrices, $\mathbf{C}_s$ and $\mathbf{C}_{\text{aer}}$ are the damping matrices, $\mathbf{K}_s$ and $\mathbf{K}_{\text{aer}}$ are the stiffness matrices. Moreover, $\mathcal{D}^2$ and $\mathbf{K}_\delta$ are the the differential operator that takes into account the derivatives in x (the beam element axis) and the linear stiffness matrix taking into account the actuator stiffness, respectively, that are defined as follows

$$\mathcal{D} = diag\left(\frac{\partial^2}{\partial x^2}, \frac{\partial^2}{\partial x^2}, \frac{\partial}{\partial x}, 0\right); \; \boldsymbol{K}_\delta = diag\,(0,0,\text{K}_\delta,0). \quad (2)$$

where

$$\text{K}_\delta = k_\delta + k_{act}\delta_F. \quad (3)$$

Materials Research Proceedings 33 (2023) 213-318 https://doi.org/10.21741/9781644902677-31

being k_δ the hinge stiffness per unit length and δ_F an expression of the Dirac delta function $\delta_F = \delta_d(x - l_F - l_{a1}) + \delta_d(x - l_F - l_{a2})$ that identifies the actuators position along the aileron span.

A third order Hermite interpolation function is introduced for the bending displacement w(x) and a linear interpolation function is used for the others generalized displacements; thus, the beam displacement interpolation can be written as

$$\mathbf{q}(x) = \mathbf{N}(x)\Delta. \tag{4}$$

where $\mathbf{N}(x)$ is the shape functions matrix and $\Delta = [w_i,\ \theta_i,\ \phi_i,\ \delta_i, \bar{x}_i, w_j,\ \theta_j,\ \phi_j,\ \delta_j,\ \bar{x}_j]^T$ is the generalized nodal displacement vector of the i − j beam finite element. The generalized interpolation is then substituted into the governing equations and their weak form is introduced obtaining the following compact form expression, where $\tilde{\boldsymbol{q}} = [\tilde{w} \quad \tilde{\phi} \quad \tilde{\delta} \quad \tilde{\bar{x}}]$ is the virtual displacement vector.

$$\int_L \tilde{\boldsymbol{q}}[\mathbf{M}_s + \mathbf{M}_{aer}]\ddot{\mathbf{q}}(t)dx + \int_L \tilde{\boldsymbol{q}}[\mathbf{C}_s + \mathbf{C}_{aer}]\dot{\mathbf{q}}(t)dx + \int_L \tilde{\boldsymbol{q}}[\mathbf{K}_s\mathcal{D}^2 + \mathbf{K}_\delta + \mathbf{K}_{aer}]\mathbf{q}(\mathbf{t})\mathbf{dx} = \mathbf{0}. \tag{5}$$

From the governing equations weak form the elemental mass, damping, and stiffness matrices can be obtained and are defined as follows

$$\begin{aligned}
\mathbf{M}_{el} &= \int_L \mathbf{N}^T[\mathbf{M}_s + \mathbf{M}_{aer}]\mathbf{N}dx \\
\mathbf{C}_{el} &= \int_L \mathbf{N}^T[\mathbf{C}_s + \mathbf{C}_{aer}]\mathbf{N}dx \\
\mathbf{K}_{el} &= \int_L [(\mathbf{DN})^T\mathbf{K}_s\mathbf{D} + \mathbf{N}^T\mathbf{K}_\delta + \mathbf{N}^T\mathbf{K}_{aer}]\mathbf{N}dx
\end{aligned} \tag{6}$$

Once the aeroelastic beam elemental matrices have been obtained the equivalent wing structural model can be realized in a finite element fashion assembling the matrices opportunely and according with the structural discretization. In this way the FEM governing equations are obtained and read as

$$\mathbf{M}_G\ddot{\mathbf{\Delta}}_G + \mathbf{C}_G\dot{\mathbf{\Delta}}_G + \mathbf{K}_G\mathbf{\Delta}_\mathrm{G} = 0. \tag{7}$$

where the subscript G stands for "global" (referring to the whole structure) and $\mathbf{\Delta}_\mathrm{G}$ is the unknown displacements vector. Finally, Eq. 6 can be cast in state-space form defining the dynamic matrix of the system as follows

$$\mathbf{A} = \begin{bmatrix} 0 & I \\ -\mathbf{M}_G^{-1}\mathbf{K}_G & -\mathbf{M}_G^{-1}\mathbf{C}_G \end{bmatrix}. \tag{8}$$

Thus, the stability analysis of the wing stick model can be carried out studying the eigenvalues of $\mathbf{A}$ for increasing speed values in order to identify the free-stream velocity for which the eigenvalues real part becomes positive valued.

Results

Validation analyses have been carried out on both clean Goland wing model and its modified wing-aileron configuration [5]. A preliminary convergence study has revealed that a subdivision of the

Materials Research Proceedings 33 (2023) 213-318 https://doi.org/10.21741/9781644902677-31

wing span in ten aeroelastic beam elements was enough for the flutter analysis of the clean Goland wing. Fig. 4 shows the Goland wing eigenvalues real part and frequency evolution with the airstream speed at sea level density, from which it can be seen that the classical coupling between the first fundamental bending and torsion modes is present for a flutter speed and frequency of $v_f = 137.4\ m/s$ and $\omega_f = 11.2\ Hz$, respectively. These results are in good agreement with the exact solution given by Goland and Luke and with other literature results that use similar approaches, as shown in Table 1.

Table 1 - Goland wing flutter results comparison

REFERENCE	MODELING APPROACH	$v_f[m/s]$	$\%E(v_f)$	$\omega_f[Hz]$	$\%E(\omega_f)$
GOLAND AND LUKE [6]	Analytical	137.25	-	11.25	-
PROPOSED APPROACH	Aeroelastic beam FE	137.40	0.1	11.10	1.33
[5]	Euler – Bernoulli beam + Strip theory (p-k method)	137.01	0.2	11.14	0.99
[7]	Intrinsic beam + strip theory	135.60	1.2	11.17	0.07
[8]	Slender beam+ modified strip theory	137.40	0.1	11.10	1.33
[9]	Thin walled beam + strip theory	137.40	0.1	11.04	1.86

For further validation the so called "heavy" version of the Goland wing has been considered [10]. In detail a structural model made up from 2D shell elements that model a box structure of spars, ribs and skin panels and 1D bar elements that model spars and ribs caps, has been implemented in Patran/Nastran, while its equivalent beam model has been realized with the aeroelastic beam approach here proposed. From the aerodynamic point of view, the heavy Goland wing structural model realized in Patran/Nastran has been completed with a DLM lifting surface with a discretization of 75 panel spanwise and 30 panels chordwise that ensure convergence of flutter results; thus, the structure/aerodynamics coupling has been provided by means of a Finite Plate Spline FPS. From the analysis carried out in Nastran it has been noted that, at sea level air density, the heavy Goland wing also presents the bending torsion modes coupling at the flutter speed $v_f^{HG}{}_{Nastran} = 119\ m/s$, shown in Fig.2.

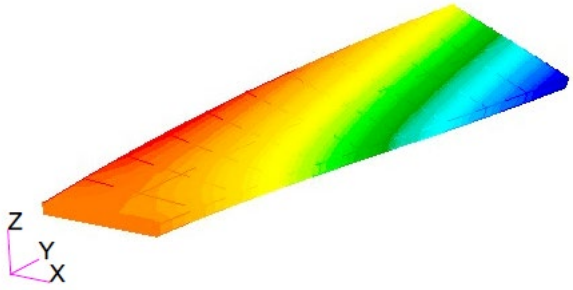

Figure 2 – Heavy Goland wing flutter mode $\omega_f^{HG}{}_{Nastran} = 2.6\ Hz$

The aeroelastic analysis of the heavy Goland wing model has been then carried out with the proposed aeroelastic beam approach considering a discretization of ten beam finite elements and the results obtained are shown in Fig. 3 where it can be seen that the predicter flutter boundary is $v_f^{HG} = 129\ m/s$ and the flutter frequency is $\omega_f^{HG} = 3\ Hz$. Due to strip theory assumptions the

Materials Research Proceedings 33 (2023) 213-318 https://doi.org/10.21741/9781644902677-31

predicted flutter speed slightly overestimates the one computed with the more accurate DLM model, but it is worth to be said that the aeroelastic beam approach has allowed to significantly reduce the problem degrees of freedom with respect to the Nastran model. In fact, the Nastran model has 4 896 DoF while its equivalent stick model presents 40 DoF only.

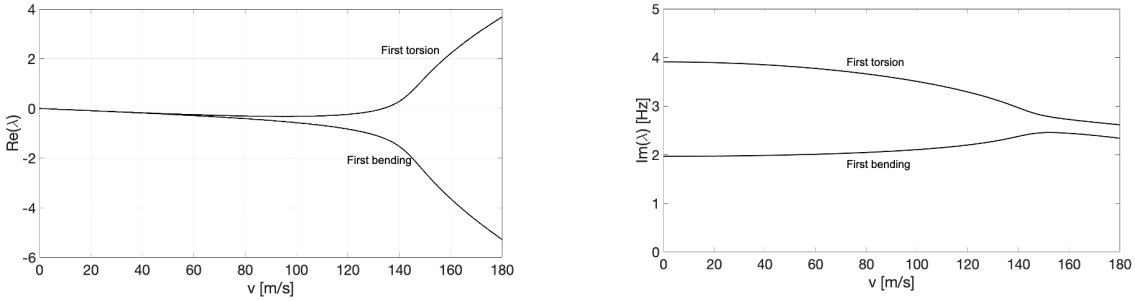

a) Eigenvalues real part b) Eigenvalues imaginary part

Figure 3. Heavy Goland wing aeroelastic analysis results

Last, the validation for a wing-aileron configuration has been carried out considering the Goland wing equipped with an aileron-type control surface extending from the 60% of the span to the wing tip. The wing-aileron stick model has been implemented considering four aeroelastic beam elements for the clean wing portion, where the flap degree of freedom has been suppressed, and six elements for the wing portion equipped with the aileron. Flutter results, in terms of eigenvalues real part and frequencies, are reported in Fig. 4 where it can be seen that, in accordance with literature results [5], the instability arises for the first wing torsion mode at the flutter speed of $v_f = 109.5\ m/s$ and frequency of $\omega_f = 10.3\ Hz$.

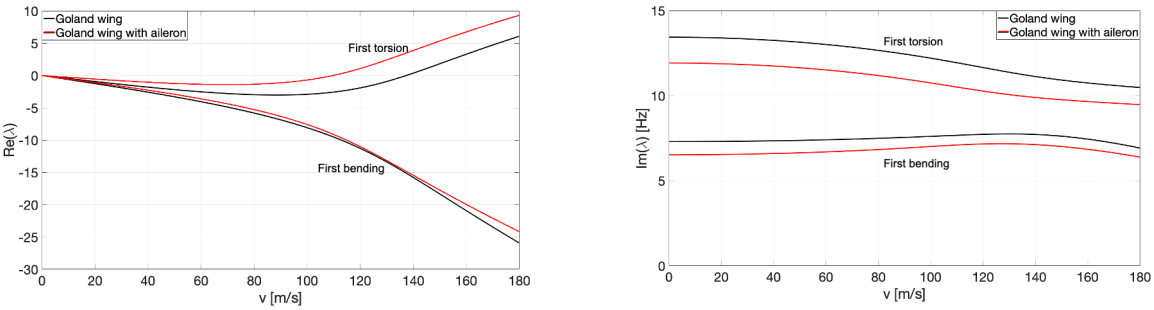

c) Eigenvalues real part d) Eigenvalues imaginary part

Figure 4. Goland wing aeroelastic analysis results

Conclusions

An alternative aeroelastic beam approach for time domain aeroelastic analysis of wing structures has been presented in this work. The flexural-torsional equivalent beam model governing equations of a wing equipped with an aileron-like control surface have been used to compute the finite element matrices by means of a weak formulation approach. Then, the obtained elemental matrices have been implemented in a beam finite element code to realize the wing numerical model and to carry out the stability analysis. Validation analyses have been carried out for clean wing configurations and for a wing with a trailing edge control surface; a comparison of the results obtained using the aeroelastic beam approach with literature and commercial code results has been provided.

References

[1] Theodorsen, T. (1949). General theory of aerodynamic instability and the mechanism of flutter (No. NACA-TR-496).

[2] Albano, E., & Rodden, W. P. (1969). A doublet-lattice method for calculating lift distributions on oscillating surfaces in subsonic flows. AIAA journal, 7(2), 279-285. https://doi.org/10.2514/3.5086

[3] Vindigni, C. R., & Orlando, C. (2022). Simple adaptive v-stack piezoelectric based airfoil flutter suppression system. Journal of Vibration and Control, 10775463221085854. https://doi.org/10.1177/10775463221085854

[4] Vindigni, C. R., Mantegna, G., Esposito, A., Orlando, C., & Alaimo, A. (2022). An aeroelastic beam finite element for time domain preliminary aeroelastic analysis. Mechanics of Advanced Materials and Structures, 1-9. https://doi.org/10.1080/15376494.2022.2124333

[5] Mozaffari-Jovin, S., Firouz-Abadi, R. D., & Roshanian, J. (2015). Flutter of wings involving a locally distributed flexible control surface. Journal of Sound and Vibration, 357, 377-408. https://doi.org/10.1016/j.jsv.2015.03.044

[6] Goland, M., & Luke, Y. L. (1948). The flutter of a uniform wing with tip weights. J. Appl. Mech. Mar 1948, 15(1),pp. 13-20. https://doi.org/10.1115/1.4009753

[7] Patil, M. J., Hodges, D. H., & Cesnik, C. E. (2000). Nonlinear aeroelastic analysis of complete aircraft in subsonic flow. *Journal of Aircraft*, *37*(5), 753-760. https://doi.org/10.2514/2.2685

[8] Berci, M., & Cavallaro, R. (2018). A hybrid reduced-order model for the aeroelastic analysis of flexible subsonic wings—A parametric assessment. *Aerospace*, *5*(3), 76. https://doi.org/10.3390/aerospace5030076

[9] Z. Qin and L. Librescu, Dynamic aeroelastic response of aircraft wings modeled as anisotropic thin-walled beams, Journal of Aircraft 40 (2003), pp. 532–543. https://doi.org/10.2514/2.3127

[10] Beran, P. S., Khot, N. S., Eastep, F. E., Snyder, R. D., & Zweber, J. V. (2004). Numerical analysis of store-induced limit-cycle oscillation. *Journal of Aircraft*, *41*(6), 1315-1326. https://doi.org/10.2514/1.404